



Calhoun: The NPS Institutional Archive
DSpace Repository

Theses and Dissertations

1. Thesis and Dissertation Collection, all items

1968

Convective precipitation amounts.

Oakes, Dudley Glen

Monterey, California. Naval Postgraduate School

<http://hdl.handle.net/10945/11868>

Downloaded from NPS Archive: Calhoun



<http://www.nps.edu/library>

Calhoun is the Naval Postgraduate School's public access digital repository for research materials and institutional publications created by the NPS community. Calhoun is named for Professor of Mathematics Guy K. Calhoun, NPS's first appointed -- and published -- scholarly author.

Dudley Knox Library / Naval Postgraduate School
411 Dyer Road / 1 University Circle
Monterey, California USA 93943

NPS ARCHIVE
1968
OAKES, D.

CONVECTIVE PRECIPITATION AMOUNTS

DUDLEY GLEN OAKES

DUDLEY KNOX LIBRARY
NAVAL POSTGRADUATE SCHOOL
MONTEREY CA 93943-5101

CONVECTIVE PRECIPITATION AMOUNTS

by

Dudley Glen Oakes
Lieutenant, United States Navy
B.A.E. , Auburn University, 1961



Submitted in partial fulfillment of the
requirements for the degree of

MASTER OF SCIENCE IN METEOROLOGY

from the

NAVAL POSTGRADUATE SCHOOL
June 1968

968
DAKES, D.

~~0.5~~
~~C.1~~

ABSTRACT

Areas of convective precipitation were delineated and averaged convective precipitation amounts determined within these areas. A statistical, step-wise, screening, linear regression procedure was used to correlate certain large scale parameters with the convective precipitation amounts.

Of the parameters considered in the two cases investigated, the best predictor of convective precipitation was either the terrain-induced vertical motion at the top of the boundary layer, or the product of the latter and the specific humidity at the same level.

TABLE OF CONTENTS

Section	Page
List of Tables	5
List of Illustrations	7
Acknowledgment	8
1. Introduction	9
2. Procedure	11
3. Results of case studies	15
4. Conclusions and remarks	29
5. Bibliography	31

LIST OF TABLES

Table		Page
1.	Matrix showing the simple correlation coefficients between the variables for Case A.	21
2.	Matrix showing the simple correlation coefficients between the variables for Case B.	21
3.	Results of step-wise regression analysis for Case A.	22
4.	Results of step-wise regression analysis for Case B.	23
5.	Regression equations using only one variable.	24
6.	Matrix showing the simple correlation coefficients between the variables, computed for the beginning of the time period, for Case A.	24
7.	Matrix showing the simple correlation coefficients between the variables, computed for the beginning of the time period, for Case B.	25
8.	Regression equations using only one variable, which was computed for the beginning of the time period.	25
9.	Improved regression equations using only one variable.	26

LIST OF ILLUSTRATIONS

Figure		Page
1.	Surface synoptic situation for 1200 GMT 11 February, 1965.	19
2.	Surface synoptic situation for 0000 GMT 12 February, 1965.	19
3.	Surface synoptic situation for 1200 GMT 16 March, 1965.	20
4.	Surface synoptic situation for 0000 GMT 17 March, 1965.	20
5.	Observed convective precipitation for Case A.	27
6.	Computed convective precipitation for Case A.	27
7.	Observed convective precipitation for Case B.	28
8.	Computed convective precipitation for Case B.	28

ACKNOWLEDGMENT

My gratitude is extended to Professor M. B. Danard for numerous helpful suggestions and criticisms during the course of this research, and whose work was the basis of this study.

1. INTRODUCTION

The failure of numerical models to account for convective precipitation is well known (see, e.g., Danard (1966 a, 1966 b)). Such a shortcoming is expected since the equations used for numerical prediction are not applicable to sub-synoptic scale motion. Convective precipitation is highly variable in both time and space. This would prevent such precipitation from being accurately accounted for even with a much denser observational network than the one available in the United States today.

This investigation is an attempt to delineate the areas of convective precipitation by the use of semi-empirical methods. Convective precipitation will be interpreted here as the average amount associated with sub-synoptic scale systems over a square area whose side is equal to the distance between adjacent grid points used in numerical prediction (381 kilometers at 60 degrees north). The amount defined is assumed to be determined by the large-scale properties of the atmosphere.

Convective activity is confined to areas of unstable, or conditionally unstable, lapse rates. That is, the lapse rate should be steeper than the moist adiabatic lapse rate. Kuo (1965) describes a convective cloud model which will "bring surface air to all levels up to a great height so that inside the cloud the vertical distribution of temperature and mixing ratio are those of the moist

adiabat through the appropriate condensation level."

This suggests that the rate of production of cloud and total water content would depend on the specific humidity, or mixing ratio, and the vertical velocity at some lower boundary. Ooyama (1963) assumed that the rate of precipitation was proportional to the flux of water vapor through the top of the frictional boundary layer. The total gain of water vapor in an air column, assuming no flux through the top of the column, may be represented by

$$I = 1/g \int_{p_b}^{p_r} \nabla \cdot q V dp - (\omega_b q_b)/g, \quad (1)$$

(e.g., Krishnamurti (1968)), where I is the water gained, q is the specific humidity, and p is pressure. The subscripts b and t indicate the bottom and top of the column, respectively. Here the first term represents the flux of water vapor through the sides of a column of unit area, and the second term represents the flux through its base, which is taken here as the top of the planetary boundary layer. Since specific humidity decreases rapidly with height, the second term is frequently larger than the first if the level p_b is sufficiently high.

2. PROCEDURE

For the two case studies included here, Danard (1966b) has made numerical predictions of gridpoint precipitation within an area shown in Figures 5-8. Predicted amounts obtained from the first 12 hours of these integrations were assumed to represent precipitation effects of large-scale motions. Observed precipitation amounts were obtained by averaging all individual values reported by synoptic stations over a square centered on the grid point and having a side equal to the distance between adjacent grid points (approximately 381 kilometers). Convective precipitation amounts used are the difference between the averaged observed amounts and the amounts predicted by Danard. Only those points where the lapse rate was close to, or greater than, the pseudo-adiabatic value (see below) were used. The maximum 12-hour precipitation amount predicted by the numerical scheme in these areas was only 0.4 millimeters in either case study. Thus, the areas of convective precipitation were clearly delineated from those of large-scale precipitation.

A statistical, step-wise, linear regression procedure was used to correlate convective precipitation with the following parameters: (1) the difference between the pseudo-adiabatic and the computed lapse rates ($\Gamma_w - \Gamma$), (2) the vertical velocity (ω) at the top of the boundary layer, (3) specific humidity (q) at the top of the boundary

layer, (4) the product of (2) and (3), and (5) dew point depression ($T - T_d$) in the lower troposphere. The program used is available in the Naval Postgraduate School computer library, where it is listed as BMD02R. A sequence of multiple linear regression equations is computed in a step-wise manner. At each step the variable is added which makes the greatest reduction in the error sum of squares.

For the two cases considered, average temperatures and dew-point temperatures were computed for the 850, 700, and 500 mb levels. The reported values at the beginning and end of the period were used to compute time averages. These averaged temperatures were used in the computations.

All averaged parameters were computed from values reported by the stations. The resulting fields were then analyzed, and the values for the grid points used were taken from the analysis.

As used here, the lapse rate is defined to be the difference between the temperatures at 850 and 500 mb. The pseudo-adiabatic lapse rate between 850 and 500 mb was taken from an Arowagram as a function of the temperature at 700 mb. Convective precipitation was considered possible where the difference between the lapse rates ($\Gamma_w - \Gamma$) was less than $2.0^{\circ}\text{C}/(350 \text{ mb})$. The areas delineated by this criterion included all regions where large amounts of convective precipitation was observed in both cases.

The dew point depression used was averaged between 850 and 700 mb. Here the 500 mb level was omitted because, in both cases many stations reported motor-boating at that level. In the cases where motor-boating was reported at the lower levels, the minimum dew point depression for which a radiosonde normally reports motor-boating was used.

Danard (1966a) expressed the vertical velocity at the top of the boundary layer as

$$\omega = \omega_r + \omega_f \quad , \quad (2)$$

where ω_r and ω_f are the vertical velocity induced by orographic and eddy-stress influences, respectively. In the area considered in this study (see Figure 1) most of the terrain heights are less than 400 meters above sea level. Therefore, the surface geostrophic wind was taken to be that at 1000 mb. Thus, ω_r is well approximated by

$$\omega_r = (V_g)_{1000} \cdot \nabla P_t \quad , \quad (3)$$

where p_t is the standard atmosphere pressure at the elevation of the smoothed terrain provided by Berkofsky and Bertoni (1955), and $(V_g)_{1000}$ is the geostrophic wind at 1000 mb.

The frictionally induced vertical velocity was computed by

$$\omega_f = g/\alpha_f (K \cdot \nabla \times C_d V_g V_g) \quad (4)$$

Here V_g is a representative geostrophic wind in the planetary boundary layer and C_d is the drag coefficient (Cressman (1960)). In the cases considered here $(V_g)_{1000}$ was used. However, over higher terrain, or in cases where $(V_g)_{1000}$ cannot be easily computed, $(V_g)_{850}$ might be more useful.

Specific humidity at the top of the boundary layer may be expressed as

$$q = \frac{0.622 e}{p - 0.378 e} \quad (5)$$

where e is the vapor pressure and p is the pressure in mb at the top of the boundary layer, assumed to be 850 mb here. Vapor pressures used were the saturation values (Smithsonian Institution (1951)) corresponding to the dew point temperatures at 850 mb.

3. RESULTS OF CASE STUDIES

Two synoptic situations were investigated: 1200 GMT 11 February to 0000 GMT 12 February, 1965, and 1200 GMT 16 March to 0000 GMT 17 March, 1965. These intervals will be referred to as Cases A and B, respectively. The surface synoptic situation for the beginning and end of the two 12 hour periods may be seen in Figures 1-4. Both cases were characterized by deepening cyclones moving from the southwest. These storms produced some of the worst weather of the 1965 winter in the central United States.

The number of grid points used in Cases A and B (i.e., the sample sizes) was 16 and 17, respectively. Tables 1 and 2 give the simple correlation coefficients between all the variables used for Cases A and B, respectively. In both cases the correlation between ω and ω_q was very high. In Case A, ω_q had the highest simple correlation with convective precipitation (P). For Case B, the correlation between ω and P was slightly higher than that between ω_q and P. The second highest simple correlation for Case A was between $(T-T_d)$ and P. However, there was little or no correlation between these variables in Case B.

The results of the step-wise regression analysis may be seen in Tables 3 and 4 for Cases A and B, respectively. In the step-wise regression procedure, the first variable

entered is always the one with the highest simple correlation with P, unless the "deletion option" of the step-wise regression program is invoked. In Case A, after ωq entered the regression equation, ω was essentially redundant and did not enter the equation at all. For the same reason ωq did not enter the equation in Case B, since ω entered first. In both cases there was little improvement in the multiple correlation between the predicted value and P after the first variable entered the regression equation.

An attempt was made to determine if a time delay between the flux of moisture through the boundary layer and resulting precipitation could be detected. To accomplish this, the regression procedure was repeated using variables computed for the beginning, rather than for the average, of the time period. The resulting simple correlation coefficients are given in Table 6 and 7. In Case A, there was noticeable improvement in the correlation between both ωq and P, and ω and P. However for Case B there was little change in these correlations.

The step-wise regression program used permits the variable ωq to enter the regression equation first for Case B if the variable ω is deleted. In this way it is possible to obtain the variable ωq as the primary predictor for both Cases A and B. In a similar manner, ω

has been selected as the primary predictor for Case A. The resulting equations, with only one variable entered, may be seen in Table 5. Due to the high simple correlation between ω and ω_q there is little loss in explained variance for either case, when ω or ω_q is employed as the primary predictor.

In order to improve the prediction equations and to ensure that $P \geq 0$, predictions were made for both cases using the equation

$$\begin{aligned} P &= A_0 + A_1(\omega_q), \text{ for } \omega_q < -A_0/A_1 \\ &= 0, \text{ for } \omega_q \geq -A_0/A_1 \end{aligned} \quad (6)$$

The coefficients A_0 and A_1 were determined by computing the quantity

$$S^2 = \sum (P_{ob} - P)^2, \quad (7)$$

where the summation extends over all the points in the sample. P_{ob} is the observed convective precipitation at a gridpoint and P is the amount given by Equation (6). S^2 is simply the error sum of squares. Various values of A_0 and A_1 were tried until the minimum in S^2 was found. This procedure was repeated using ω as the predictor. The improved prediction equations are shown in Table 9. Comparing the last columns of Tables 5 and 9, it is seen that the above procedure results in a slight reduction in error for Case B. However, for Case A the improvement is negligible.

Predictions were made for both cases using the equation

$$\begin{aligned} P &= -0.45 - 1.20(\omega q) , \text{ for } \omega q < -0.375 \\ &= 0 , \text{ for } \omega q \geq -0.375 . \end{aligned} \quad (8)$$

Equation (8) was obtained by averaging the coefficients given in the first two lines of Table 9. The results may be compared with the observed convective precipitation in Figures 5-8.

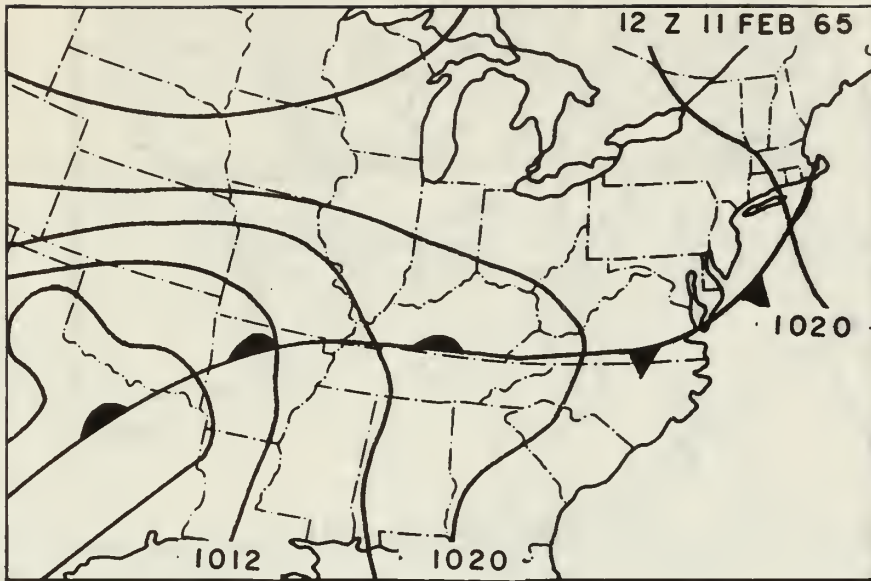


Figure 1

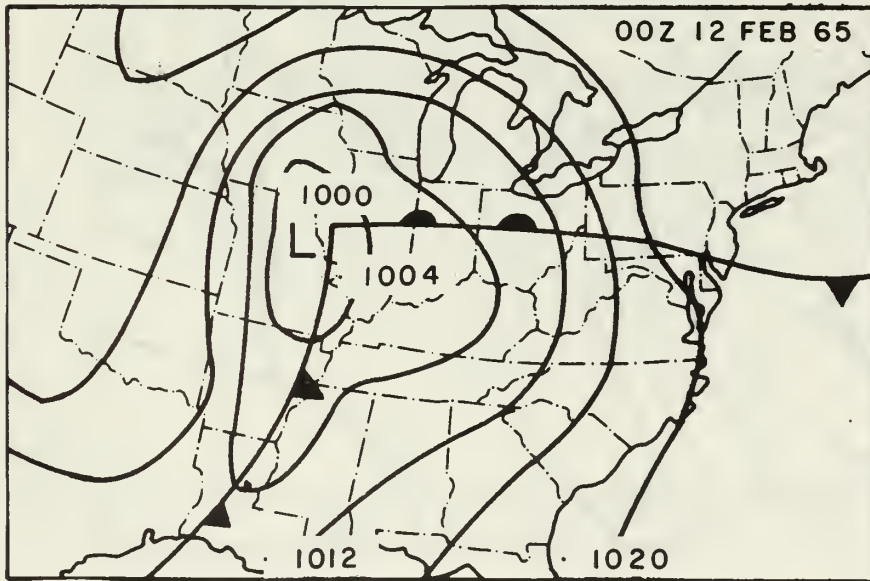


Figure 2

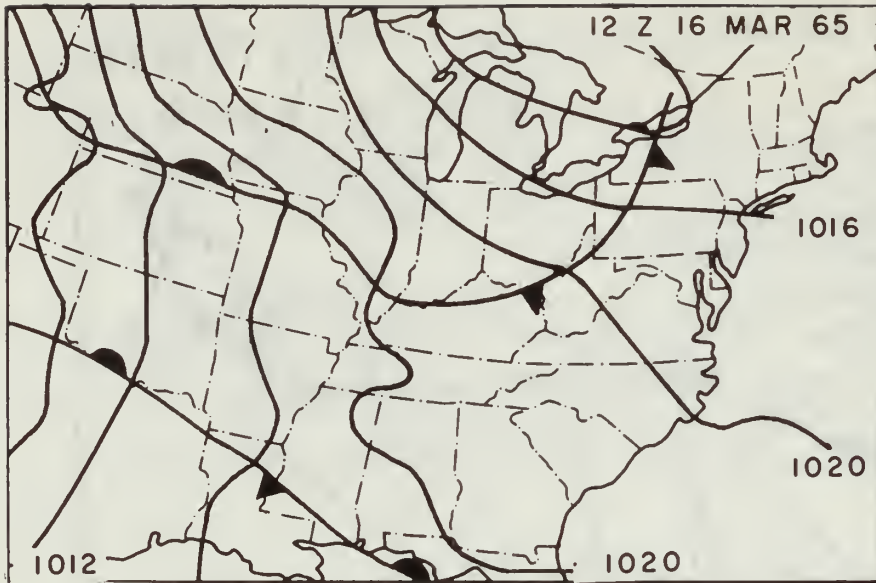


Figure 3

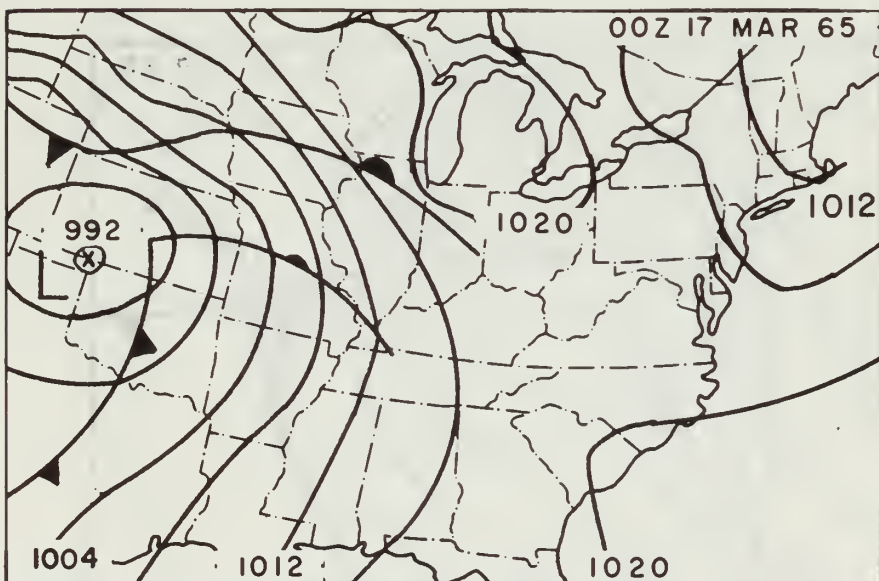


Figure 4

TABLE I

Matrix showing the simple correlation coefficients between the variables for Case A, P is convective precipitation.

	P	$\Gamma_w - \Gamma$	ω	q	ωq	$T - T_d$
P	1.00	0.28	-0.43	0.12	-0.51	-0.47
$\Gamma_w - \Gamma$		1.00	-0.34	-0.13	-0.35	-0.44
ω			1.00	-0.10	0.95	0.55
q				1.00	-0.28	0.01
ωq					1.00	0.53

TABLE II

Same as Table I for Case B

	P	$\Gamma_w - \Gamma$	ω	q	ωq	$T - T_d$
P	1.00	-0.25	-0.67	-0.24	-0.65	-0.08
$\Gamma_w - \Gamma$		1.00	0.01	-0.65	-0.01	-0.34
ω			1.00	0.45	0.98	0.31
q				1.00	0.48	0.36
ωq					1.00	0.28

TABLE III

Results of step-wise regression analysis for Case A in the form of regression equations. $P = A_0 + \sum A_i V_i$, where P is the precipitation in mm/12 hr, and V_i is the variable entered at the i step. R is the multiple correlation coefficient between P and the predictand at the i step.

Step	Variable entered	Units	R	A_0	Regression coefficients				Root mean square error of estimate (mm/12 hr)
					A_1	A_2	A_3	A_4	
1	ωq	dynes $\text{cm}^{-2} \text{sec}^{-1}$	0.51	0.57	-1.66				4.65
2	$T - T_d$	$^{\circ}\text{C}$	0.56	4.73	-1.20	-0.41			4.48
3	$P_w - P$	$^{\circ}\text{C}/350\text{mb}$	0.56	4.47	-1.17	-0.39	-0.30		4.47
4	q	gm/kg	0.56	3.73	-1.14	-0.39	-0.33	-0.13	4.47

NOTE: ωq is multiplied by 10^3

TABLE IV

Same as Table III for Case B.

Step	Variable entered	Units	R	A_0	Regression coefficients				Root mean square error of estimate (mm/12 hr)
					A_1	A_2	A_3	A_4	
1	ω	dynes cm ⁻² sec ⁻¹	0.67	-0.08	-1.37				1.28
2	$\Gamma_w - \Gamma$	°C/350mb	0.72	-0.33	-1.36	-0.17			1.21
3	q	gm/kg	0.74	1.18	-1.12	-0.30	-0.31		1.18
4	$T - T_d$	°C	0.74	0.76	-1.16	-0.28	-0.31	0.04	1.18

TABLE V

Regression equations using only
the first variable entered.

Case	Variable entered	R	Regression coefficients		Root mean square error of estimate
			A_0	A_1	
A	ωq	0.51	0.57	-1.66	4.65
B	ωq	0.65	-0.01	-0.32	1.32
A	ω	0.43	1.07	-9.20	4.89
B	ω	0.67	-0.08	-1.37	1.28

TABLE VI

Matrix showing the simple correlation
coefficients between the variables for
Case A. The primed variables were computed
for the beginning of the time period.

	P	$\Gamma_w - \Gamma$	ω'	q'	$\omega'q'$	$T' - T'_d$
P	1.00	0.28	-0.65	0.04	-0.64	-0.10
$\Gamma_w - \Gamma$		1.00	-0.24	-0.39	-0.14	-0.30
ω'			1.00	-0.40	0.99	0.36
q'				1.00	-0.42	-0.62
$\omega'q'$					1.00	0.33

TABLE VII

Same as Table VI for Case B

	P	$\Gamma_w - \Gamma$	ω'	q'	$\omega'q'$	$T' - T'_d$
P	1.00	-0.25	-0.62	-0.11	-0.66	0.37
$\Gamma_w - \Gamma$		1.00	0.06	-0.64	0.04	-0.04
ω'			1.00	0.44	0.93	-0.32
q'				1.00	0.41	0.01
$\omega'q'$					1.00	-0.26

TABLE VIII

Same as Table V for variables
computed for the beginning of
the time period.

Case	Variable entered	R	Regression coefficients		Root mean square error of estimate
			A_0	A_1	
A	$\omega'q'$	0.64	1.71	-2.08	4.16
B	$\omega'q'$	0.66	0.21	-0.72	1.31
A	ω'	0.65	2.22	-13.77	4.14
B	ω'	0.62	0.07	-2.59	1.36

TABLE IX

Improved regression equations using
only the first variable entered.

Case	Variable entered	Regression coefficients		Root mean square error of estimate
		A_0	A_1	
A	ωq	0.20	-1.80	4.63
B	ωq	-1.10	-0.50	1.19
A	ω	1.00	-0.35	4.88
B	ω	-0.80	-1.85	1.20

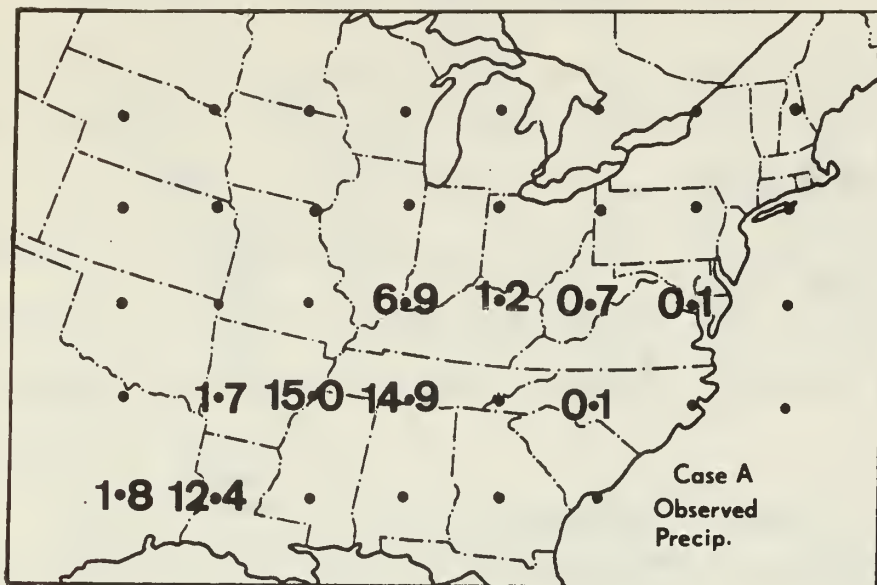


Figure 5

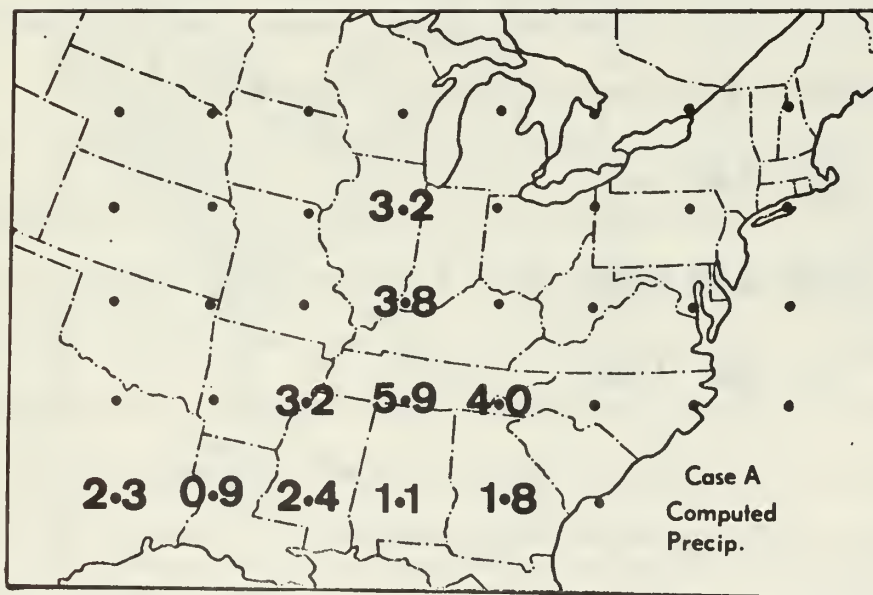


Figure 6

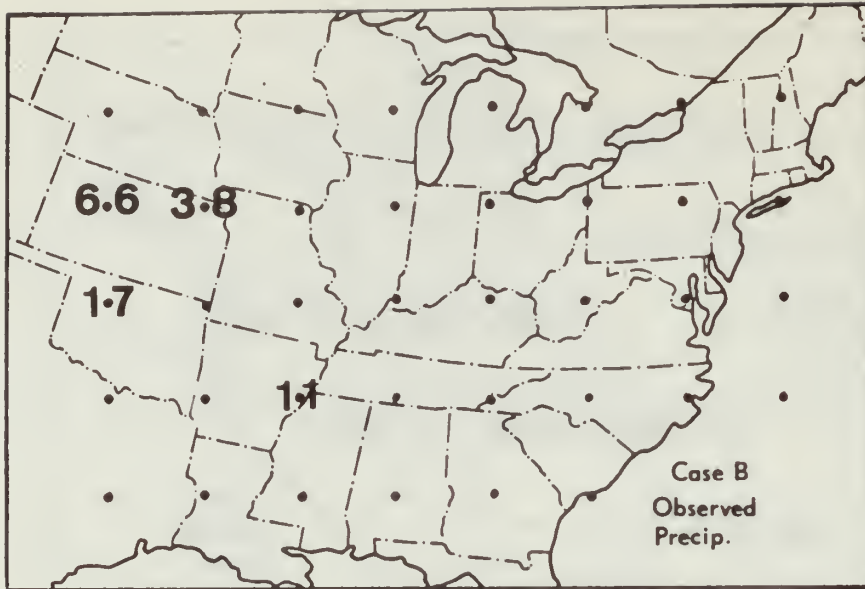


Figure 7

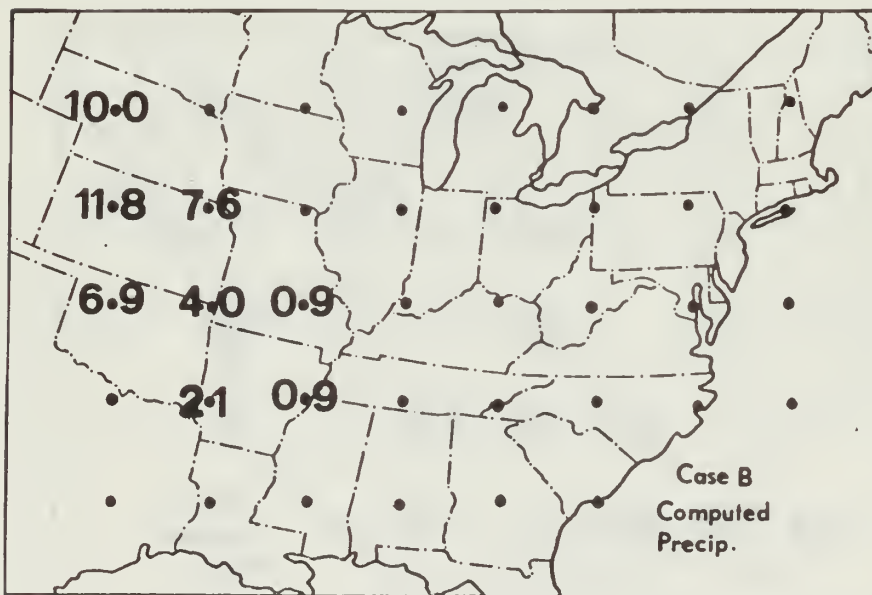


Figure 8

4. CONCLUSIONS AND REMARKS

Probably the most that could be claimed for the results of this study is that it may have some applicability over the central and eastern United States for the winter months during the period 1200 to 0000 GMT. However there is indication that the product of vertical velocity and specific humidity at the top of the boundary layer can be used to predict convective precipitation.

While this study is diagnostic in nature, it uses data that can be predicted numerically. Consequently, the technique could be included in a prognostic scheme with some expectation of success. The technique of using lapse rates, as described here, to determine areas of possible convective activity could be applied to local forecast areas using forecast temperature fields.

For a synoptic situation to be used in this type of a study, there must be a clear delineation between large-scale and convective precipitation. To find out if a situation meets this requirement, a prediction of precipitation amounts due to large-scale processes must be made and compared to the reported precipitation. The time required for this procedure limited this study to the two cases considered here. Furthermore, the small size of the samples virtually precludes a statistical

proof of the significance of the results. However, the findings of this study are sufficiently encouraging to justify further work.

BIBLIOGRAPHY

- 1) Berkofsky, L., and E. A. Bertoni, 1955: Mean topographical charts of the entire earth, Bulletin of the American Meteorology Society, vol. 36, pp. 350-354.
- 2) Cressman, G. P., 1960: Improved terrain effects in barotropic forecast, Monthly Weather Review, vol. 88, pp. 327-342
- 3) Danard, M. B., 1966a: A quasi-geostrophic numerical model incorporating effects of release of latent heat, Journal of Applied Meteorology, vol. 5, pp. 85-93.
- 4) _____, 1966b: Further studies with a quasi-geostrophic numerical model incorporating effects of released latent heat, Journal of Applied Meteorology, vol. 5, pp. 388-395
- 5) Krishnamurti, T. N., 1968: A calculation of percentage area covered by convective clouds from moisture convergence, Journal of Applied Meteorology, vol. 7, pp. 184-195.
- 6) Kuo, H. L., 1965: On formation and intensification of tropical cyclones through latent heat release by cumulus convection, Journal of the Atmospheric Sciences, vol. 22, pp. 40-63.
- 7) Ooyama, K., 1963: A dynamic model for the study of tropical cyclone development, Department of Meteorology and Oceanography, New York University, 26 pp.
- 8) Smithsonian Institution, 1951: Smithsonian Meteorological Tables, 6th rev. ed., prepared by R. J. List. Washington, pp. 351-395.

INITIAL DISTRIBUTION LIST

	No. Copies
1. Lt. Dudley G. Oakes PATRON Eleven FPO New York, New York 09501	1
2. Professor Maurice Danard Department of Mechanical Engineering University of Waterloo Waterloo, Ontario, Canada	2
3. Library Naval Postgraduate School Monterey, California 93940	2
4. Department of Meteorology & Oceanography Naval Postgraduate School Monterey, California 93940	3
5. Defense Documentation Center Cameron Station Alexandria, Virginia 22314	20
6. Officer in Charge Naval Weather Research Facility Naval Air Station, Building R-48 Norfolk, Virginia 23511	1
7. Officer in Charge Fleet Numerical Weather Facility Naval Postgraduate School Monterey, California 93940	1
8. Commanding Officer Fleet Weather Central Navy Department Washington, D. C. 20390	1
9. AFCRL - Research Library L. G. Hanscom Field Attn: Nancy Davis/Stop 29 Bedford, Massachusetts 01730	1
10. Superintendent Naval Academy Annapolis, Maryland 21402	1

- | | | |
|-----|---|---|
| 11. | Director, Naval Research Laboratory
Attn: Tech. Services Info. Officer
Washington, D. C. 20390 | 1 |
| 12. | Department of Commerce, ESSA
Weather Bureau
Washington, D. C. 20235 | 1 |
| 13. | Professor T. N. Krishnamurti
Department of Meteorology
Florida State University
Tallahassee, Florida 32303 | 1 |
| 14. | Office of Naval Research
Department of the Navy
Washington, D. C. 20360 | 1 |

DOCUMENT CONTROL DATA - R & D

(Security classification of title, body of abstract and indexing annotation must be entered when the overall report is classified)

1. ORIGINATING ACTIVITY (Corporate author) Naval Postgraduate School Monterey, California 93940		2a. REPORT SECURITY CLASSIFICATION	
		2b. GROUP	
3. REPORT TITLE Convective Precipitation Amounts			
4. DESCRIPTIVE NOTES (Type of report and inclusive dates)			
5. AUTHOR(S) (First name, middle initial, last name) Dudley Glen Oakes			
6. REPORT DATE 21 Jun 1968		7a. TOTAL NO. OF PAGES 33	7b. NO. OF REFS 8
8a. CONTRACT OR GRANT NO.		9a. ORIGINATOR'S REPORT NUMBER(S)	
b. PROJECT NO.			
c.		9b. OTHER REPORT NO(S) (Any other numbers that may be assigned this report)	
d.			
10. DISTRIBUTION STATEMENT This document is subject to special export controls and each transmittal to foreign governments or foreign nationals may be made only with prior approval of NPGS.			
11. SUPPLEMENTARY NOTES		12. SPONSORING MILITARY ACTIVITY Naval Postgraduate School Monterey, California 93940	
13. ABSTRACT <p>Areas of convective precipitation were delineated and averaged convective precipitation amounts determined within these areas. A statistical, step-wise, screening, linear regression procedure was used to correlate certain large scale parameters with the convective precipitation amounts.</p> <p>Of the parameters considered in the two cases investigated, the best predictor of convective precipitation was either the terrain-induced vertical motion at the top of the boundary layer, or the product of the latter and the specific humidity at the same level.</p>			

14

KEY WORDS

LINK A

LINK B

LINK C

ROLE

WT

ROLE

WT

ROLE

WT

Convective Precipitation



—

thes015

Convective precipitation amo

DUDLEY KNOX LIBRARY



3 2768 00421966 7

DUDLEY KNOX LIBRARY